bioRxiv preprint doi: https://doi.org/10.1101/2022.11.04.514813; this version posted November 4, 2022. The copyright holder for this preprint (which was not certified by peer review) is the author/funder, who has granted bioRxiv a license to display the preprint in perpetuity. It is made available under aCC-BY-ND 4.0 International license.

Microplastics are present in follicular fluid and compromise gamete function *in vitro*: Is the Anthropocene throw-away society throwing away fertility?

Authors

Nicole Grechi[1], Roksan Franko[1,2], Roshini Rajaraman[2], Jan B. Stöckl[3], Tom Trapphoff[4], Stefan Dieterle[4,5], Thomas Fröhlich[3], Michael J. Noonan[6], Marcia de A. M. M. Ferraz[1,2]*

[1]Clinic of Ruminants, Faculty of Veterinary Medicine, Ludwig-Maximilians University of Munich, Sonnenstr. 16, Oberschleissheim, 85764, Germany

[2]Gene Center, Ludwig-Maximilians University of Munich, Feodor-Lynen Str. 25, Munich, 81377, Germany

[3]Laboratory for Functional Genome Analysis, Gene Center, Ludwig-Maximilians University of Munich, Feodor-Lynen Str. 25, Munich, 81377, Germany

[4] Dortmund Fertility Centre, Olpe 19, 44135 Dortmund, Germany

[5]Division of Reproductive Medicine and Infertility, Department of Obstetrics and Gynecology, Witten/Herdecke University, Alfred-Herrhausen-Str. 50, Witten, 58455, Germany

[6]The Irving K. Barber School of Sciences, The University of British Columbia, Okanagan Campus, Kelowna, BC V1V 1V7, Canada

*Corresponding author: E-mail: m.ferraz@lmu.de

Abstract

Decades of careless use and improper disposal have resulted in plastic pollution accumulating almost everywhere on earth, yet the health implications of the billions of tons of plastic pollution scattered across the planet's terrestrial ecosystems are largely unknown. We show that microplastics are present in the follicular fluid of women and domestic cows. We found that the concentrations of microplastics that naturally occurred in follicular fluid were sufficient to compromise the normal functioning of both male and female bovine gametes *in vitro*. Proteomics analysis of oocytes further revealed how microplastic can disrupt the expression of proteins associated with normal oocyte function. Microplastics also negatively affected sperm function *in vitro*. Collectively, these findings demonstrate how microplastics may be contributing to the widespread declines in fertility that have been occurring over recent Anthropocene decades.

Keywords

Infertility, follicular fluid, oocyte biology, sperm function, plastic pollution, toxicity.

bioRxiv preprint doi: https://doi.org/10.1101/2022.11.04.514813; this version posted November 4, 2022. The copyright holder for this preprint (which was not certified by peer review) is the author/funder, who has granted bioRxiv a license to display the preprint in perpetuity. It is made available under aCC-BY-ND 4.0 International license.

Introduction

Decades of careless use and improper disposal have resulted in plastic pollution accumulating almost everywhere on earth[1,2] and microplastics (MPs) – defined as plastic particles <5 mm in size that are insoluble in water – have now been documented in even the most remote environments[3–5]. The exponentially increasing volume of plastic pollution making its way into rivers, lakes and oceans has drawn considerable scientific, public[6–8], and governmental attention[9]. However, despite the tens of thousands of peer reviewed publications on plastic pollution, an overwhelming majority of these have focused on aquatic ecosystems, and very little is known about the effects of MPs in terrestrial systems[10]. This knowledge gap is made all the more noteworthy by the fact that 80% of the Earth's species live on land[11] and terrestrial systems may represent a larger environmental reservoir of MPs than oceans[12,13]. With the plastic pollution crisis only expected to worsen over the coming decades[14], it is imperative that we improve our understanding of the potential health effects of the tens of billions of tons of plastic pollution that litter the globe.

While any health effects are undesirable, the potential impacts of MPs on reproductive systems are of particular concern. Reproduction is central to the capacity for species to maintain stable populations. Poor reproductive health not only reduces individual fecundity but, if widespread, species survival. Over the past several decades there has been an alarming increase in the rates of reproductive dysfunctions and gamete abnormalities, reductions in gamete production, and altered embryo development in humans, animals and plants[15–23]. While the overarching cause of these worrying declines in fertility has yet to be identified, emerging studies are showing that MPs represent a potentially serious threat to the reproductive health of terrestrial species[13,24–26]. Data have been limited to studies on laboratory animals, however, and the extent to which they are representative of the conditions that animals are actually experiencing in their natural environment is unknown. Consequently, it is unclear to what extent MPs can bio-accumulate in free-ranging terrestrial mammals and influence fertility. Here, we assessed the extent to which MPs might be bio-accumulating in the follicular fluid of women and domestic cows. Particles isolated from human and bovine follicular fluid were identified via Raman spectroscopy, and the composition of particles were adjusted to those found in water controls. We then investigated the effects of MPs on bovine male and female gametes *in vitro* at concentrations within the biological detection range. With human activity around the globe already having triggered the sixth major episode of mass extinction[27–29], understanding the long-lasting effects of plastics on reproductive systems is essential for developing the tools and strategies needed to combat the plastic pollution crisis and ensure the future of life on Earth.

Results

MPs, pigments, and plasticizers in human and cow follicular fluid

MPs were found in all human (hFF) and bovine follicular fluid (bFF) samples, with a mean concentration of 17.8 and 38.1 particles mL^{-1}, respectively. A high amount of undigested matter was detected in the samples by an automated analysis of the sample membranes using the Particle Scout software (ranging from 4,912 total particles in water control 2 to 40,683 total particles in bFF3; Fig. 1A). Despite these large numbers of particles, only 8,863, 4,523, 1,122, 265, 476, 3,893, 355, 605, 382 and 604 particles for hFF1, hFF2, hFF3, bFF1, bFF2, bFF3, waters 1, 2, 3 and 4, respectively, had Raman spectra with hit quality index (HQI) ≥ 75. Figure 1B shows examples of plastic polymers identified in FF and their spectra match. The total number of MP particles varied substantially between samples, with a total of 42.5 particles mL^{-1} in hFF1, 9.2 particles mL^{-1} in hFF2, 1.6 particles mL^{-1} in hFF3, 6.8 particles mL^{-1} in bFF1, 17.1 particles mL^{-1} in bFF2 and 91.8 particles mL^{-1} in bFF3 (Fig. 1C; Table S1). Non-plastic related particles were the majority of identified particles (27.8 to 75.3 %), while MP polymers accounted for 0.8 to 23.5 % of total identified particles. Other plastic-related particles that were identified included pigments

bioRxiv preprint doi: https://doi.org/10.1101/2022.11.04.514813; this version posted November 4, 2022. The copyright holder for this preprint (which was not certified by peer review) is the author/funder, who has granted bioRxiv a license to display the preprint in perpetuity. It is made available under aCC-BY-ND 4.0 International license.

(0 to 3.6 %), plasticizers (2.0 to 50.9 %), and coating, solubilizers and fillers (2.8 to 20.7 %; Fig. 1D). A total of 24 different MP polymers were identified, with the most abundant being rubber in humans and polyvinyl chloride in bovine. The sizes of the MPs in hFF ranged from 3.6 to 48.1 µm in length (mean±SD = 12.7±8.7 µm) and 2.1 to 38.4 µm in width (mean±SD = 7.8±5.6 µm). The sizes of the MPs in bFF ranged from 3.07 to 49.4 µm in length (mean±SD = 11.4±7.2 µm) and 1.7 to 27.8 µm in width (mean±SD = 6.7±4.0 µm). Based on their sizes and densities, we determined that MPs summed to 0.0309 µg mL^{-1} in hFF1, 0.0032 µg mL^{-1} in hFF2, 0.0002 µg mL^{-1} in hFF3, 0.0009 µg mL^{-1} in bFF1, 0.005 µg mL^{-1} in bFF2 and 0.069 µg mL^{-1} in bFF3. Of importance for the present study, polystyrene in hFF1 equalled to 0.0005 µg mL^{-1}, in bFF3 equalled to 0.0126 µg mL^{-1} and to 0.00035 µg mL^{-1} in bFF2, while it was not identified in hFF2, hFF3 and bFF1. Full details on the particles contained in each of the samples are shown in Data S1 and plastic polymer particles are summarized in Table S1 .

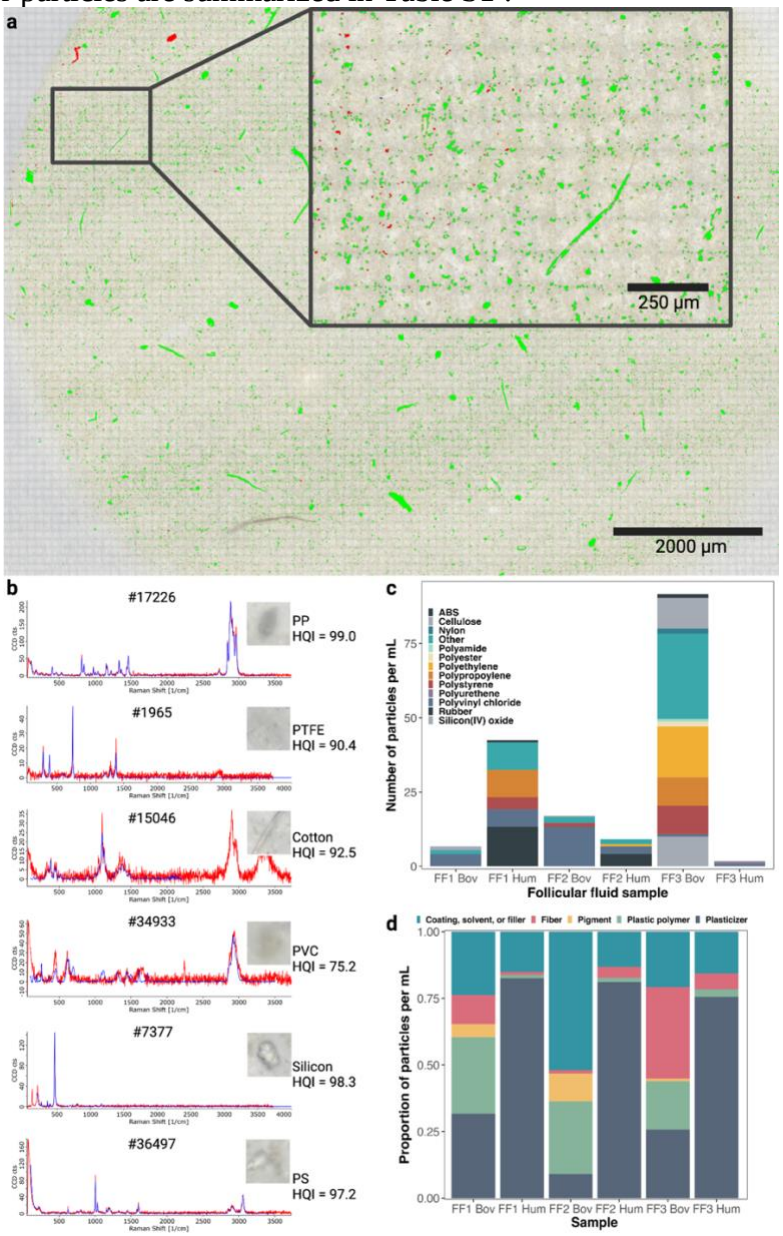

Fig. 1. MPs were detected in bovine follicular fluid. In (**A**), an example of an imaged membrane (bFF3) that was used in the software Particle Scout to determine the number of particles

bioRxiv preprint doi: https://doi.org/10.1101/2022.11.04.514813; this version posted November 4, 2022. The copyright holder for this preprint (which was not certified by peer review) is the author/funder, who has granted bioRxiv a license to display the preprint in perpetuity. It is made available under aCC-BY-ND 4.0 International license.

and their sizes and for subsequent spectra match using the software TrueMatch is shown. Particles shown in green represent all counted particles, while those shown in red represent particles for which the spectra match had a hit quality index (HQI)≥ 75. In (**B**) examples of plastic polymer particles from bFF3 with their Raman spectra (red) and the matched Raman spectra of the corresponding plastic polymer (blue) from the ST Japan and/or SLoPP database. Particle number, polymer name and HQI are shown. In (**C**) the composition of MPs detected in human (hum) and bovine (bov) follicular fluid by confocal Raman spectroscopy are shown. In (**D**) the counts of the different plastic and non-plastic analysed particles present in each sample are shown. The number of MPs in (**C**) was adjusted to the number of particles detected in their respective water control. PP = polypropylene, PTFE = polytetrafluoroethylene, PVC = polyvinylchloride, PS = polystyrene.

MPs reduce oocyte maturation and induce damage of the zona pellucidae

In order to evaluate the effects of MPs on *in vitro* oocyte maturation, we counted the number of oocytes with broken zona pellucida, that were degenerating, and that were mature (Fig. 2A). *In vitro* maturation performed in the presence of polystyrene beads resulted in a significantly lower number of mature oocytes in comparison to the control group (control: 68.1±10.3%, 0.3 µm MPs: 42.0±14.8%, and 1.1 µm MPs: 41.0±17.6%; $p < 0.00001$ for both 0.3 and 1.1 µm MPs; Fig. 2A), with no significant difference between the 0.3 and 1.1 µm MP treatments ($p = 0.963$). The number of degenerated oocytes varied between 27% and 37% and did not differ between any of the groups, however the control group had significantly fewer oocytes with broken zona pellucidae when compared to the groups incubated with MPs (control: 4.4±5.2%, 0.3 µm MPs: 21.4±7.6%, and 1.1 µm MPs: 26.2 ±10.9%; $p < 0.0001$ for all groups). Notably, of the oocytes with broken zona pellucidae 80% were mature in the control group, as compared to 40 and 35%, for the 0.3 and 1.1 µm MP treatments, respectively, but these oocytes were categorised as having broken zona pellucidae, and not as mature.

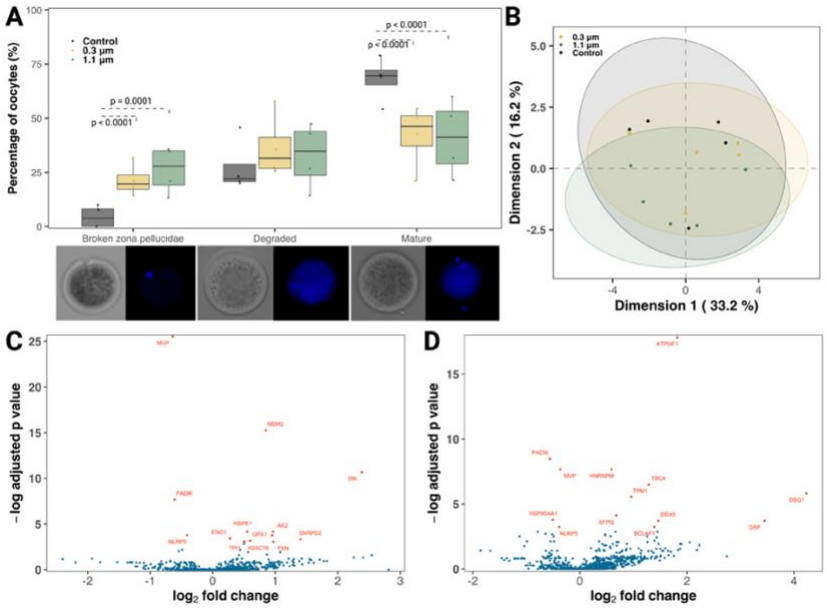

Fig. 2. Polystyrene MPs negatively influenced oocyte maturation. The boxplots in (**A**) show the effects of 24 h exposure to 0.3 and 1.1 µm polystyrene beads on oocyte maturation *in*

bioRxiv preprint doi: https://doi.org/10.1101/2022.11.04.514813; this version posted November 4, 2022. The copyright holder for this preprint (which was not certified by peer review) is the author/funder, who has granted bioRxiv a license to display the preprint in perpetuity. It is made available under aCC-BY-ND 4.0 International license.

vitro. Image examples of each stage characterization below the panel, oocytes were stained for DNA (Hoechst33342, blue). The scatter plot in (**B**) depicts the first two dimensions (Dim) of a principal component analysis (PCA) across the proximity matrix of a random forest model classifying oocytes exposed to 0.3 or 1.1 µm polystyrene beads versus the control, based on protein expression profiles. Volcano plots depicting differently expressed proteins between oocytes incubated for 24 h in the presence of (**C**) 0.3 µm and (**D**) 1.1 µm polystyrene beads compared to a control are also shown.

MPs alter the oocyte proteome

A total of 2,060 proteins were identified across all oocyte samples and a low variance was observed between the different groups (Fig. 2B). A total of 153 proteins were unique to oocytes incubated with 0.3 µm beads, 724 to those incubated with 1.1 µm beads, and 261 to the control oocytes, while 730 proteins were common to all treatment groups (Fig. S1). We found that 13 proteins were present at significantly different abundances when comparing oocytes incubated with 0.3 µm polystyrene beads and control (3 down-regulated and 10 up-regulated). Likewise, the abundances of 13 proteins were significantly different in oocytes incubated with 1.1 µm polystyrene beads compared to the control (4 down-regulated and 9 up-regulated; Fig. 2C and D; Table 1).

Table 1. Differentially abundant proteins in oocytes incubated with or without polystyrene MPs. Protein name and ID, gene name, fold change and adjusted P-value are shown for oocytes incubated with 0.3 µm polystyrene beads compared to control and oocytes incubated with 1.1 µm polystyrene beads compared to the control. The full list of identified differentially abundant proteins is available in Data S2.

Comparison	Protein name and ID	Gene name	Fold change	Adj. p-value
0.3 µm vs control	Major vault protein (Q3SYU9)	MVP	0.6	8.2E-12
	Malate dehydrogenase, mitochondrial (Q32LG3)	MDH2	1.8	2.3E-07
	Acyl-CoA-binding protein (P07107)	DBI	5.2	2.3E-05
	Protein-arginine deiminase (F1N404)	PADI6	0.7	4.6E-04
	Adenylate kinase 2 (P08166)	AK2	2.0	1.5E-02
	10 kDa heat shock protein, mitochondrial (P61603)	HSPE1	1.5	1.5E-02
	NACHT, LRR and PYD domains-containing protein 5 (Q647I9)	NLRP5	0.8	2.3E-02
	Glutathione peroxidase 1 (P00435)	GPX1	1.9	2.3E-02
	Alpha-enolase (Q9XSJ4)	ENO1	1.2	3.2E-02
	Small nuclear ribonucleoprotein Sm D2 (Q3SZF8)	SNRPD2	2.6	3.6E-02
	H2A clustered histone 16, 7, 14, 10, 17 (A0A3Q1N7K2)	H2AC16; H2AC7; H2AC14; H2AC10; H2AC17	1.5	4.2E-02
	Triosephosphate isomerase (Q5E956)	TPI1	1.4	4.5E-02
	Thioredoxin (O97680)	TXN	2.0	4.7E-02
1.1 µm vs control	ATPase inhibitor, mitochondrial (P01096)	ATP5IF1	3.5	1.8E-08
	Protein-arginine deiminase (F1N404),	PADI6	0.7	2.1E-04
	Major vault protein (Q3SYU9)	MVP	0.8	4.7E-04

bioRxiv preprint doi: https://doi.org/10.1101/2022.11.04.514813; this version posted November 4, 2022. The copyright holder for this preprint (which was not certified by peer review) is the author/funder, who has granted bioRxiv a license to display the preprint in perpetuity. It is made available under aCC-BY-ND 4.0 International license.

	Heteroous nuclear ribonucleoprotein (A0A3Q1MJD5)	HNRNPM	1.5	4.7E-04
	Tubulin-specific chaperone A (P48427)	TBCA	2.4	1.5E-03
	Desmoglein-1 (Q03763)	DSG1	18.8	3.0E-03
	Tropomyosin alpha-1 chain (Q5KR49)	TPM1	1.9	3.9E-03
	Splicing factor proline and glutamine rich (E1BQ37)	SFPQ	1.6	1.6E-02
	Heat shock protein HSP 90-alpha (Q76LV2)	HSP90AA1	0.7	2.3E-02
	Probable ATP-dependent RNA helicase (F1MBQ8)	DDX5	2.8	2.4E-02
	Desmoplakin (E1BKT9)	DSP	10.9	2.4E-02
	BCL2 associated transcription factor 1 (F1MQU4)	BCLAF1	2.6	3.9E-02
	NACHT, LRR and PYD domains-containing protein 5 (Q647I9)	NLRP5	0.8	3.9E-02

MPs attach to the sperm surface but are not internalized

Due to the physical limitations of light microscopy and Raman spectroscopy, only the larger 0.3 and 1.1 µm polystyrene beads were analysed for attachment. For polystyrene beads these sizes, we observed that sperm incubated in the presence of the 0.3 µm beads had a higher number of beads attached to the surface than those incubated with the 1.1 µm beads ($p < 0.001$; Fig. 3A). We also found that the percentage of sperm with attached MP beads did not change over time ($p = 0.3$). From our microscopy analyses, we found no evidence of polystyrene beads being internalized by the sperm cells.

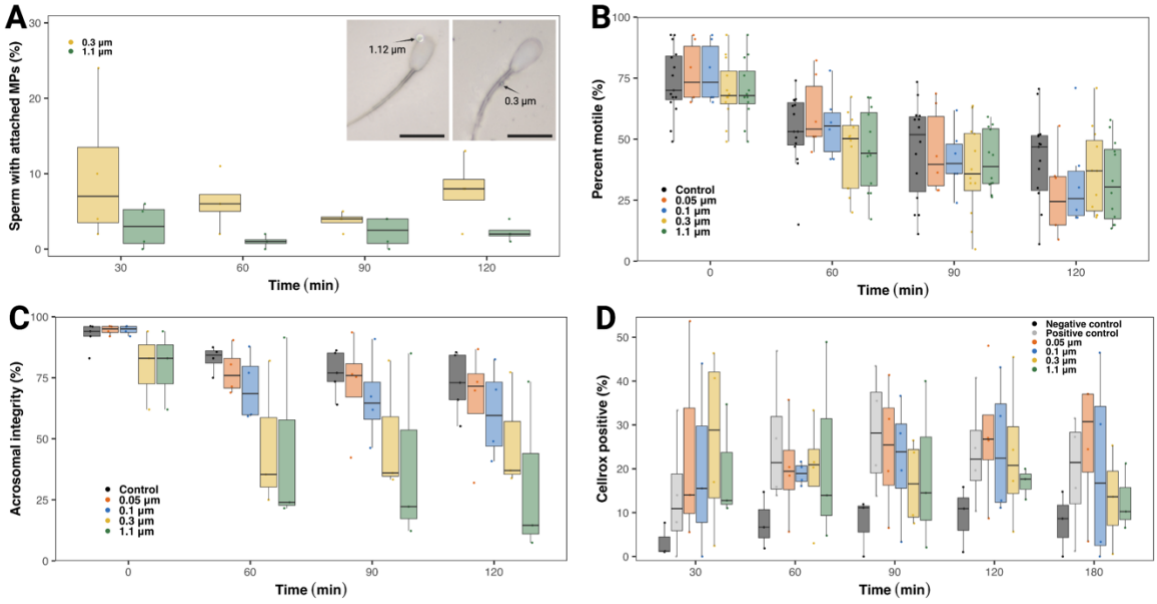

Fig. 3. Polystyrene MP effects on sperm function *in vitro*. (**A**) Percentage of sperm cells with polystyrene beads attached to their surface over time with picture examples of 0.3 and 1.1 µm attached beads. Attachment did not change over time, and beads were not internalized by the spermatozoa, but the 0.3 µm beads attached more to the sperm surface than the 1.1 µm beads ($p = 0.003$). Scale bars in the insets have a length of 10 µm. Boxplot depicting (**B**) the lack of any effect of polystyrene MPs of different sizes on sperm motility, (**C**) the significant reduction in acrosome integrity in all groups, independently of the size of the bead ($p<0.001$), and (**D**) the increased production in reactive oxygen species in all MPs groups when compared to the negative control, with 0.05 and 0.1 µm beads reaching levels similar to the positive control.

bioRxiv preprint doi: https://doi.org/10.1101/2022.11.04.514813; this version posted November 4, 2022. The copyright holder for this preprint (which was not certified by peer review) is the author/funder, who has granted bioRxiv a license to display the preprint in perpetuity. It is made available under aCC-BY-ND 4.0 International license.

MPs induce acrosome damage and oxidative stress but have no influence on sperm motility

Sperm motility decreased over time ($p < 0.001$), but, irrespective of their size, the polystyrene beads did not induce significant changes in sperm motility when compared to the control group (Fig. 3B). Nonetheless, it was observed that the presence of MPs, independent of size, negatively impacted acrosome integrity when compared to the negative control (Fig. 3C, $p < 0.001$). Finally, we also observed that polystyrene beads significantly increased reactive oxygen species production at all time points compared to the negative control (Fig. 3D). The presence of the smaller 0.05 and 0.1 μm beads induced the production of reactive oxygen species to levels that were comparable to the positive control, which was stimulated with hydrogen peroxide, a known cellular reactive oxygen species inducer. The larger 0.3 and 1.1 μm beads also induced higher oxidative stress compared to the negative control ($p = 0.02$, and $p = 0.036$ respectively), although not to the same extent as the positive control, as was seen in sperm exposed to the 0.05 and 0.1 μm beads.

Discussion

The ubiquitous and long-lived nature of MPs has made them synonymous with the seemingly irreversible mark of mankind on our planet. While evidence is still extremely limited, emerging studies are showing that MPs represent a potentially serious threat to the reproductive health of laboratory rodents and aquatic species[13,24,36,25,26,30–35]. Due to the lack of a reliable method for isolating and characterising MPs from biological tissues and fluids, however, our capacity to investigate the presence of MPs in naturally occurring biological samples has been limited. In addition, there were heretofore no studies linking MP contamination to changes in fertility in non-lab-rodent terrestrial mammals. This study provides the first comprehensive evaluation of the detrimental effects of MPs contamination on the mammalian reproductive system. Using a protocol that was optimized for the isolation of small MPs from FF, we have shown that MPs are present in the FF of women and domestic bovine. From our *in vitro* analyses, we found that the concentrations of MPs that occurred in domestic bovine FF were shown to compromise the normal functioning of male and female bovine gametes. Collectively, these findings provide evidence as to how the billions of tons of MP pollution may be contributing to the widespread increase in the rates of reproductive dysfunctions that have been increasing over recent decades[15–23].

To perform a bio-mimetic experiment investigating the impact of MPs on fertility (and health in general) *in vitro,* it is necessary to have baseline information about what type, size, and amount of MPs can plausibly bio-accumulate in humans and other terrestrial mammals. In reality, no such information is currently available. This can be attributed to two main reasons: 1) the vast majority of MPs research has focused on aquatic ecosystems, and 2) due to cost, time, and technological limitations there are no reliable methods for isolating, characterizing and quantifying small MPs (<10 μm) from complex biological samples. In an attempt to overcome the latter limitation, we optimized a protocol that allowed the analysis of MPs in cow and human FF samples. Nevertheless, there was still a large amount of undigested substances in the samples. Although this allowed for the detection of MP particles in FF, it resulted in the protocol requiring 3-7 days per sample to acquire the Raman spectra of all the detected particles, in addition to 4-18 hours to match these to the database. While this protocol was sufficient for the scale of the present study, it is clearly not a viable option for large scale applications. Showing that the refinement of methodologies for the sampling, detection, and quantification of MPs from biological samples is critical for the future of the field[43–45].

Using confocal Raman spectroscopy, we detected 7 major MPs (17.8 particles mL^{-1} or 0.011 μg mL^{-1}; polyvinyl chloride – PVC, polyethylene – PE, polystyrene – PS, polypropylene – PP, polyurethane – PU, rubber – RUB, and ABS) in human follicular fluid. While in bFF 10 major MPs (38.6 particles mL^{-}

bioRxiv preprint doi: https://doi.org/10.1101/2022.11.04.514813; this version posted November 4, 2022. The copyright holder for this preprint (which was not certified by peer review) is the author/funder, who has granted bioRxiv a license to display the preprint in perpetuity. It is made available under aCC-BY-ND 4.0 International license.

^{1} or 0.025 μg mL^{-1}; PVC, PE, cellulose – CE, PS, PP, silicon – SL, nylon – NL, polyester – PES, ABS and polyamide – PA) were detected. The number of MPs we found in human and bovine FF were more than what was detected in human placentae (0.52 particles g^{-1}; PE, PP and Polyurethane – PU), human lungs (0.69 particles g^{-1}; PP, polyethylene terephthalate – PET, Polytetrafluoroethylene – PTFE, PS, polyacrylonitrile – PAN, polymethyl methacrylate – PMMA and PU), and raw cow milk (4.1 particles mL^{-1}; PE, PES, PP, PTFE, PU and PA)[39,46–48] via particle spectroscopy. However, the concentration of MPs in human and bovine FF were less than that of polymers identified in human blood (1.6 μg mL^{-1}; PET, PE, PE and PMMA), cow raw milk (~18.1 μg mL^{-1}; PVC, PP, PE, PS and PMMA), cow blood (~5.4 μg mL^{-1}, PVC, PP, PE, PS and PMMA), and cow meat (~420.5 μg mL^{-1}, PVC, PP, PE, PS and PMMA)[49,50] via pyrolysis – gas-chromatography/mass-spectroscopy (Py-GC/MS). Such differences are likely due to the fact that, by using spectroscopy, we were limited to the size of particles we could analyse, and Raman spectroscopy was probably under-estimating the number of MPs. While the analysis of MPs by Py-GC/MS can detect particles down to monomers, which is more sensitive to the amount of plastics, but it comes with the trade-off of not being able to determine the size and shapes of particles. This latter information can be critical for understanding the potential for MPs to cross biological barriers.

From the total 0.011 μg mL^{-1} of MPs we detected in hFF and 0.025 μg mL^{-1} of MPs we detected in bFF, 0.00079 and 0.0043 μg mL^{-1}, or 6.9 and 17.3%, were PS, for hFF and bFF, respectively. Similarly, 13% (0.7 μg g^{-1}) of MPs detected in cow blood were PS, while cow meat (5.11%; 21.5 μg g^{-1}), and milk (0.11%; 0.02 μg g^{-1}) had a reduced amount of PS polymers[50]. In human blood, PS was the major detected polymer (60%; 0.96 μg mL^{-1})[49]. As seen for human and bovine blood, bovine milk and meat, the total amount of MPs detected is extremely variable between individuals and animal origin. Here, we have shown that, similarly to other body fluids and to tissues, MPs are also present in human and bovine follicular fluid. Nonetheless, it is still unknown to what extent the amount of MPs in FF might correlate with the amount of MPs in less invasive blood and/or stool samples, which would be an interesting topic of future research.

While the present work is not the first study on the effects of MPs on mammalian reproduction, it is the first to demonstrate the effects of MPs at concentrations that fall within the range of MPs detected in reproductive fluids. For instance, in a recent study where mice were fed 30 mg kg^{-1} of body weight of PS MPs for 35 days, the amount of PS MPs detected in blood (135.86 μg mL^{-1}), was 141 and 194 times higher than the PS MPs and 85 and 25 times higher than the total MPs in human and cow blood, respectively[51]. Those authors found that MPs can accumulate in ovaries and cause increased oxidative stress and reduced oocyte maturation[51], but they detected PS MPs in mouse ovarian tissue at a concentration of 62.6 μg g^{-1} [51], which was 79,240 and 14,558 times higher than the amount of PS MPs in hFF and bFF, respectively. Likewise, it was 5,690 and 2,504 times higher than the total amount of MPs we detected in hFF and bFF, respectively. Similarly, mice fed with 15 – 1,500 μg of polystyrene day^{-1} for 90 days, exhibited a reduced ovarian follicle reserve, ovarian oxidative stress, granulosa cell apoptosis, and ovarian fibrosis[32]. While the results from these studies are certainly alarming, the extent to which they are representative of the conditions animals are actually experiencing in the real world is questionable. Using values in the range of MPs detected in bFF (0.0178 – 0.929 μg mL^{-1}; 24 h), we demonstrated that MPs undesired effects on oocytes can actually be seen at dramatically lower concentrations of MPs exposure and within a much shorter incubation time. Crucially, the discrepancy between the concentrations of MPs used in existing studies versus those that humans and animals can experience in the environment, emphasises the dire need to better understand how and where terrestrial animals and humans bioaccumulate MPs. This information would provide a more realistic picture of the impact of MP

bioRxiv preprint doi: https://doi.org/10.1101/2022.11.04.514813; this version posted November 4, 2022. The copyright holder for this preprint (which was not certified by peer review) is the author/funder, who has granted bioRxiv a license to display the preprint in perpetuity. It is made available under aCC-BY-ND 4.0 International license.

pollution on terrestrial ecosystems, and allow researchers to establish baseline levels of exposure for *in vitro* experiments on the impact of MPs on health and fertility.

Beyond these functional responses, proteomics analysis of oocytes incubated with or without microplastic also revealed proteins altered in abundance that are part of critical oocyte function pathways (Fig. 4). Proteins that are known to act upon oxidative stress were up-regulated in the presence of MPs: TXN[52], GPX1[53], ATP5IF1[54] and PADI6[55,56], which together with the up-regulation of SNRPD2[57], known for promoting DNA repair response, indicate that the presence of MPs may induce oxidative stress and DNA damage in incubated oocytes during *in vitro* maturation. Proteins known to induce apoptosis, such as BCLAF1[58], TPM1[59] and AK2[60] were up-regulated in MPs incubated oocytes, while the MVP[61], a known oocyte protector, was down-regulated. Additionally, DDX5[62] was up-regulated and HSP90AA1[63] was down-regulated in the presence of MPs. Together with an up-regulation of HNRNPM[64,65] and TBCA[66], and down-regulation of PADI6[55,56], these differentially abundant proteins can provide a mechanistic explanation as to the reduced maturation rate observed in oocytes exposed to MPs, since these proteins are important for nuclear maturation, spindle formation and microtubule and organelle organization.

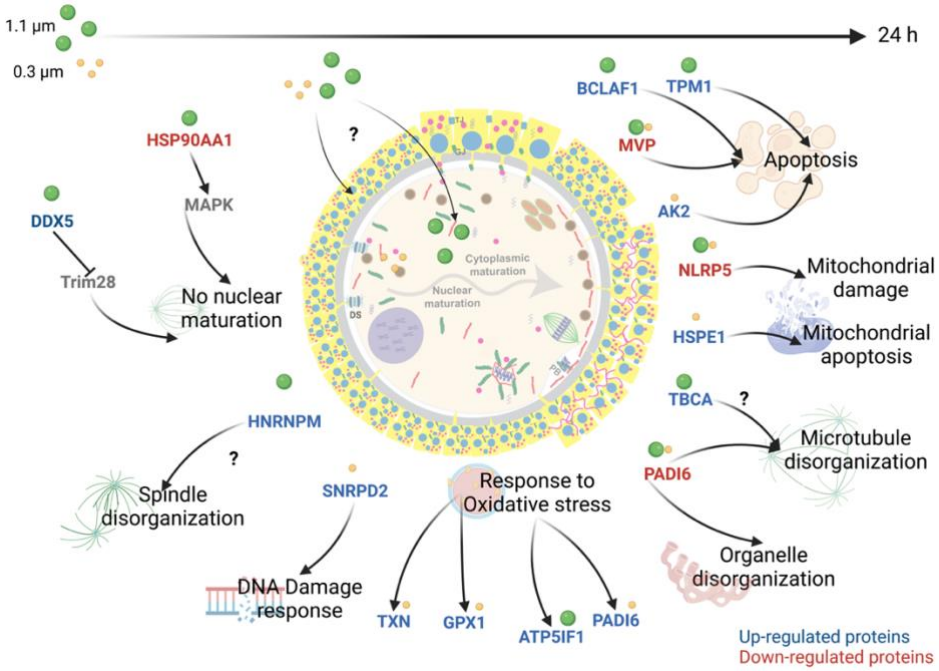

Fig. 4. Summary of polystyrene MP effects on oocyte proteomics. Differentially expressed proteins in oocytes incubated for 24 h with 0.3 (yellow) and 1.1 (green) µm polystyrene beads compared to control are shown. Proteins were found to regulate major pathways in oocyte function, such as apoptosis, mitochondrial damage, mitochondrial apoptosis, microtubule disorganization, organelle disorganization, spindle disorganization and nuclear maturation. Moreover, proteins part of response to oxidative stress and DNA damage were also differently expressed. Figure made using BioRender.

We also found that more realistic exposure to polystyrene MPs can impair male gamete function *in vitro*. Unlike in mice and rats fed with PS beads[24,30], we did not see effects of MPs on sperm motility. Here, however, sperm cells experienced a direct 2 h exposure to only 0.000083 – 0.929 µg mL^{-1} of PS,

bioRxiv preprint doi: https://doi.org/10.1101/2022.11.04.514813; this version posted November 4, 2022. The copyright holder for this preprint (which was not certified by peer review) is the author/funder, who has granted bioRxiv a license to display the preprint in perpetuity. It is made available under aCC-BY-ND 4.0 International license.

whereas in *in vivo* studies mice were exposed to 1,000 μg mL^{-1} day^{-1} for 28 days, and rats to 15 – 1,500 μg day^{-1} for 90 days. The reduced motility observed in these *in vivo* studies may also have been due to effects of MPs on the testis/epididymis, which we were not able to test via our *in vitro* exposure. Nevertheless, in accordance with existing studies, we did observe reduced acrosome integrity[24,30] and increased oxidative stress[30] in sperm exposed to MPs. It is important to note that Jin et al.[24] studied the effects of MPs on male fertility by feeding mice MPs at concentrations that were ca. 100,000 times greater than they would be exposed to in the wild[67]. Altogether, our data show that exposure to even a low concentration of polystyrene MPs for short period of time can negatively impact normal functioning of the sperm cell.

Humans and animals have been exposed to MPs for decades. The short-term effects of MPs on gametes *in vitro* we observed here are therefore likely to be more pronounced *in vivo*, due to the detrimental effects of MPs accumulating over time. It would not be surprising that MPs are contributing to the distressing increase in reproductive dysfunctions and gamete abnormalities, reductions in gamete production, and altered embryo development in humans, animals and plants over recent decades[15–22,33]. Before we can draw any broad-scale conclusions or correlations, however, it is important to note that, as previously discussed for different environmental matrices (soil, air or water), every new research must take into consideration the ubiquitous presence of numerous anthropogenic factors, of relevance here the MPs, in the environment, how they can influence the interpretation of the data and/or contaminate samples and how essential controls are for each experimental design[68].

Materials and Methods

MP contamination prevention

To prevent sample contamination with airborne/materials MPs, all procedures were performed in a laminar flow hood, and all flasks and other apparatuses were replaced by glass materials whenever possible. Moreover, all materials and equipment used were rinsed three times with filtered (0.1 μm filter – Merck Isopore) ultra-pure water prior to use. All reagents and water used in the protocols described below were also filtered using a 0.1 μm filter before use.

Microplastic polystyrene beads

Polystyrene beads (SURF-CAL™ particle size standards) having average sizes of 0.047 μm, 0.100 μm, 0.304 μm and 1.112 μm were purchased from Thermo Fisher Scientific. The beads were obtained in deionized filtered water in a concentration of 3×10^8 particles mL^{-1} and were diluted according to the concentrations required for each experiment.

Human follicular fluid collection

Follicular fluid samples were collected from patients undergoing intracytoplasmic sperm injection (ICSI) treatment between January and September 2022, at the Dortmund Fertility Centre, Germany. The study was approved by the ethics committee at Witten Herdecke University (no. S-262/2021). Briefly, aspiration of cumulus oocytes complexes (COCs) was done ultrasound-guided from large Graafian follicles after ovarian stimulation and hCG priming. The oocytes were processed for further ICSI-treatment. The extant hFF without cumulus oocytes complexes was transferred to pre-washed and sterile glass bottles (Schuett

bioRxiv preprint doi: https://doi.org/10.1101/2022.11.04.514813; this version posted November 4, 2022. The copyright holder for this preprint (which was not certified by peer review) is the author/funder, who has granted bioRxiv a license to display the preprint in perpetuity. It is made available under aCC-BY-ND 4.0 International license.

biotec, Germany) and immediately frozen at -20°C. hFF collection and processing were performed under clean room facilities.

Bovine oocyte and follicular fluid isolation

Bovine ovaries were obtained from a local slaughterhouse and immediately transported to the laboratory in a stainless-steel container at room temperature. Immature cumulus oocytes complexes (COCs) were aspirated from follicles with a size between 2 and 8 mm, together with follicular fluid, by using a vacuum pump and a 19G needle. Collected fluids with COCs from ~20-30 ovaries (N = 3 pools) were let to pellet for a maximum of 10 min. The pellet was then transferred to a petri dish with the equivalent amount of washing media (IVF Bioscience, UK) for oocyte selection, and remaining follicular fluid frozen in pre-washed glass vials at -20ºC for MPs isolation as described below. Each bFF pool was collected in a different day, each pool comprise animals coming from the same farm, and pools form different days include animals from different farms.

Microplastic isolation from human and bovine follicular fluid

Three pools of bovine follicular fluid (bFF) and follicular fluid from three human (hFF) patients, left after removal of the COCs, were used for microplastic isolation. Water controls from follicular fluid aspiration (N=2 for bFF and N=2 for hFF) were produced by, aspirating filtered ultra-pure water in the same systems that the human and bovine follicular fluids were aspirated. On day one, 2 mL of each sample were added to an Erlenmeyer for digestion in KOH 10% in a proportion of 1:25 (sample:digestion solution). The samples were incubated in a shaker at 60ºC and 250 rpm for 24 h. After this period, NaClO was added to each digestion to reach a final concentration of 7.5%, and samples were incubated for another 24 h in the shaker at 60ºC and 250 rpm. On day three, all samples were filtered in a 47 mm polytetrafluoroethylene polymer (PTFE) membrane (0.45 µm pores, Merck Millipore, USA) and rinsed with filtered ultra-pure water at least three times in order to prevent any NaClO and KOH contamination. Next, the membranes were placed in a beaker containing 50 mL of HNO_3 20% and incubated in an ultrasonic bath (TI-H-5 MF2 230 V, Elma Schmidbauer GmbH, Germany) with 100% power, sweep function and a frequency of 45 kHz for 15 min, to transfer plastics/undigested matters from the membrane into the solution. The resulting solution was then kept in the shaker at 40ºC and 250 rpm for another 24 h. At the end of the third digestion day, the samples were filtered using 13 mm PTFE membranes (0.45 µm pores) and again rinsed three times with ultra-pure filtered water. The membranes were then mounted on a glass slide for microscopy and spectroscopy analysis.

The blank control waters were processed using same protocol and in parallel to the corresponding follicular fluids, including its aspiration using same materials/equipment: water control 1 with bFF1 and bFF2 samples, water control 2 with bFF3 sample, water control 3 with hFF1 sample and water control 4 with hFF2 and hFF3 samples. Similarly, adjustment of MPs detection on FF samples to water controls (as described below) was performed using these corresponding water-FF samples combinations.

Oocyte isolation, incubation with MPs and nuclear stage analysis

After collection as described above, the Petri dish with COCs was screened with a stereomicroscope and good quality oocytes (homogeneous cytoplasm and, at least, 3 layers of cumulus cells) were selected. COCs were then washed three times in washing media, and one time in BO-IVM (IVF Bioscience, UK), before being randomly assigned to one of three incubation groups: 1) a control group containing only maturation media (N = 114); 2) media containing PS beads of size 0.304 µm (N = 93); and 3) media

bioRxiv preprint doi: https://doi.org/10.1101/2022.11.04.514813; this version posted November 4, 2022. The copyright holder for this preprint (which was not certified by peer review) is the author/funder, who has granted bioRxiv a license to display the preprint in perpetuity. It is made available under aCC-BY-ND 4.0 International license.

containing PS beads of size 1.112 μm (N = 103). The concentration of the beads in each group was 1.2 million beads mL^{-1}, or 0.0178 and 0.929 μg mL^{-1} for beads 0.3 and 1.1, respectively. The groups were cultured for 24 h in an incubator at 38.5ºC in a humidified atmosphere of 5% CO_2 and 95% O_2. After the 24 h period of incubation, the oocytes were denuded by pipetting to remove cumulus cells, washed, and either fixed in paraformaldehyde 4% for nuclear staging or frozen at -80ºC in pools of 9 oocytes for proteomics analysis (N = 5 pools per group).

For determining oocyte nuclear stage, fixed oocytes were washed in phosphate buffer saline (PBS), stained with Hoechst 33342 (5 μg mL^{-1}) for 45 min and imaged in an EVOS M7000 Microscope using a ×40 NA 1.25 objective. The oocytes were analysed for nuclear stage (metaphase 1 or 2 – determined by the presence of an aligned metaphase plate with/without a polar body, respectively), degenerated (no visible nuclear material, or pyknotic nucleus), and broken zona pellucidae (visible breaks in the zona pellucida).

Oocyte proteomics analysis

For lysis, nine oocytes per sample were sonicated in lysis buffer (8 M urea in 50 mM ammonium bicarbonate). Samples were then reduced in a final concentration of 4 mM dithiothreitol and 2 mM Tris(2-carboxyethyl)phosphine hydrochloride for 30 min at 56°C. Alkylation was done in the dark for 30 min with 8 mM iodoacetamide. Residual iodoacetamide was quenched by adding dithiothreitol to a final concentration of 10 mM. Samples were then digested in two steps, first 4 h with LysC at 37°C, then after dilution to 1 M Urea, trypsin was added and samples were digested overnight at 37°C. Prior to LC-MS/MS analysis, samples were dried using a centrifugal evaporator and then resuspended in 0.1 % formic acid (FA). Peptides were analysed with a Q Exactive HF-X (Thermo Fisher Scientific) mass spectrometer coupled to an Ultimate 3000 RSLC chromatography system (Thermo Fisher Scientific). First, samples were trapped (PepMap 100 C18, 100 μm × 2 cm, 5 μM particles; Thermo Fisher Scientific) at a flow of 5 μL min^{-1} of 0.1 % FA. Peptides were then separated (EASY-Spray; PepMap RSLC C18, 75 μm × 50 cm, 2 μm particles, Thermo Fisher Scientific) at a flow rate of 250 ηL min^{-1} employing a two-step gradient: First ramping from 3 % B to 25 % B in 80 min then to 40 % B in 9 min (A: 0.1% FA in water, B: 0.1 % FA in acetonitrile). The mass spectrometer was run in data dependent acquisition mode with up to 15 MS/MS scans per survey scan. Raw files were processed with MaxQuant 1.6.7.0[69] using the bovine subset of both Swiss-Prot and TrEMBL (Retrieval date: 24/05/2022) as database. Additionally, the built-in common contaminants database was used. Label free quantification and match between runs was turned on. Subsequent statistical analysis was done using R (4.2.0). Differentially abundant proteins were identified with the package MS-EmpiRe[70].

Sperm incubation with MPs

Frozen bull sperm were thawed at 37ºC for 30 s. The content of the straws were added to 3 mL of Tyrode's medium supplemented with 2 mM sodium bicarbonate, 10 mM lactate, 1 mM pyruvate, 6 mg mL^{-1} fatty acid–free bovine serum albumin (BSA), 100 U mL^{-1} penicillin and 100 μg mL^{-1} streptomycin, centrifuged for 5 min at 700xg, and the pellet submitted to a standard swim-up separation using Tyrode's medium supplemented with 25 mM sodium bicarbonate, 22 mM lactate, 1 mM pyruvate, 6 mg mL^{-1} fatty acid–free BSA, 100 U mL^{-1} penicillin and 100 μg mL^{-1} streptomycin (FERT) as overlaying medium. After 1 h, the supernatant was recovered, and sperm concentration was calculated using a Neubauer chamber. A total of $5x10^6$ sperm mL^{-1} were used for incubation. For the incubation with microplastic, five treatment groups

bioRxiv preprint doi: https://doi.org/10.1101/2022.11.04.514813; this version posted November 4, 2022. The copyright holder for this preprint (which was not certified by peer review) is the author/funder, who has granted bioRxiv a license to display the preprint in perpetuity. It is made available under aCC-BY-ND 4.0 International license.

were prepared: 1) a control group of FERT media without beads; 2) FERT media containing 0.047 μm polystyrene beads; 3) FERT media containing 0.100 μm polystyrene beads; 4) FERT media containing 0.304 μm polystyrene beads; and 5) FERT media containing 1.112 μm polystyrene beads. The concentration of beads in all groups was 1.2 million beads mL^{-1} or 0.000083, 0.00066, 0.0178 and 0.929 μg mL^{-1} for beads 0.05, 0.1, 0.3 and 1.1, respectively. Sperm were incubated at 38.5ºC in a humidified atmosphere of 5% CO_2 and 95% O_2 for 2 h, and assessed for motility, acrosome integrity, and bead attachment analysis at 0, 1, 1.5 and 2 h.

Sperm motility, bead attachment, and acrosome integrity assessment

At each of the time points mentioned above, a 5 μL aliquot of sperm was placed in a pre-warmed slide, covered with a coverslip and a video of at least 5 distinct areas for motility analysis was recorded, using an EVOS M7000 (Thermo Fisher Scientific, USA) microscope; same volume was also added to a SuperFrost™ slide (Expredia), fixed with an equal volume of paraformaldehyde 4% and smeared across the slide. Those slides were left to dry at RT overnight before subsequent analysis of bead attachment and acrosome integrity. The sperm motility (N = 4 bulls) was calculated by analysing each video and counting the percentage of motile sperm. For the bead attachment, the confocal Raman microscope (WITec, Germany) was used, the slides were imaged using a ×100 DIC NA 0.9 objective, and random areas selected and analysed for the presence of sperm with microplastic attached to its surface. Each slide had at least 100 sperm cells counted (N = 4 bulls). Due to difficulties in visualizing the smallest 0.05 and 0.1 μm polystyrene beads, bead attachment was only quantified for the 0.3 and 1.1 μm beads.

For the acrosome integrity analysis (N=3 bulls), fixed slides were washed 3 times with PBS, and stained using a Hoechst 33342 (5 μg mL^{-1}, Thermo Fisher Scientific, USA) and FITC-PNA Alexa 493 (5 μg mL^{-1}, Thermo Fisher Scientific, USA) solution for 15 min. Slides were then washed another 3 times with PBS and mounted using an anti-fade solution (ProLong™ Gold Antifade Mountant, Thermo Fisher Scientific, USA) and a cover slip. The samples were imaged using a Leica Thunder Dmi8 Microscope. The stained sperm cells were visualized with a ×20 NA 1.25 objective. At least 100 sperm cells/group were counted to determine percentage of cells with intact acrosome.

Sperm oxidative stress analysis

We were also interested in assessing the extent to which bovine spermatozoa experienced oxidative stress when exposed to MPs. To this end, for all of the 5 treatment groups described above, 2 μL mL^{-1} of CellRox™ Green Reagent (Thermo Fisher Scientific, USA) was added to the FERT media (N = 4 bulls). A positive control group was also created by adding 50 μM of H_2O_2 to stimulate sperm oxidative stress[71]. Sperm were then incubated at 38.5ºC in a humidified atmosphere of 5% CO_2 and 95% O_2 for 3 h. Every 30 min, a 5 μL aliquot was taken and mounted in a RT slide and cover slip. Slides were allowed to cool down at room temperature for 1 min (to reduce sperm movement) and images were taken using an EVOS M7000 fluorescence microscope using ×20 NA 0.45. At least 100 sperm cells were counted, and midpiece CellRox™ stained sperm were considered positive.

Confocal Raman spectroscopy of isolated microparticles and polystyrene beads

A confocal Raman (alpha300 R, WITec, Germany) with a spectrometer (UHTS 300, WITec, Germany), and a 532 nm laser was used for the characterization of the microplastics. The microscope was operated

bioRxiv preprint doi: https://doi.org/10.1101/2022.11.04.514813; this version posted November 4, 2022. The copyright holder for this preprint (which was not certified by peer review) is the author/funder, who has granted bioRxiv a license to display the preprint in perpetuity. It is made available under aCC-BY-ND 4.0 International license.

by using the Control Five software, and the acquired data were processed by the Project Five software for compensation of background noise or cosmic radiation signal. Initially, the microscope was focused on the samples by using a ×50 NA 0.75 Zeiss objective, and the whole area of the membrane was imaged using the 'Area Stitching' option and the Z-stack auto-focus. Then, the Particle Scout software was used to identify all the particles present in the imaged membrane. The Raman spectra of each identified particle was then measured with a ×100 DIC NA 0.9 Zeiss objective, using an autofocus function, with a laser power of 10 mV, an accumulation of 4 and integration time of 0.45 s. The presence of microplastics was confirmed by matching the spectra found using the True Match- Integrated Raman Spectra Database Management software, with the S.T. Japan database (S.T. Japan Europe GmbH, Germany) and the SloPP MPs Raman library [72]. Only matches with a hit quality index (HQI) value higher than 75% were considered for further analysis. Poly(tetrafluoroethylene-co-perfluoro-(alkyl vinyl ether)) – PTFE – and Perfluoroalkoxy alkane – PFA – particles were excluded from the analysis, since they are components of the pore membrane used for imaging. After matching and excluding membrane particles, the number of MPs was adjusted to the particles detected in the water controls by subtracting the number of particles detected in the water controls from the number of particles in FF, for each specific polymer detected individually.

All identified particles were classified as: 1) non-plastic related particles; 2) plastic polymers; 3) plasticizers; 4) pigments; 5) coatings, solvents or fillers (CSF); 6) fiber; and 7) unknown. Data S3 show a list of all identified particles and their classification. Particle number was converted to weight by using the formula:

$$P_w = \rho \times v$$

where P_w is particle weight, ρ is the particle density, and v is the particle volume. See Table S2 for full information on the density of the particles analysed here.

To determine the potential source of the 0.3 µm and 1.1 µm polystyrene beads attached to sperm cells, the Raman spectra of identified polystyrene beads was measured with a ×100 DIC NA 0.9 Zeiss objective, with a laser power of 5 mV, an accumulation of 10 and integration time of 0.5 s. The polystyrene composition of the beads was confirmed by matching the spectra found using the True Match- Integrated Raman Spectra Database Management software, with the S.T. Japan database.

Statistical analysis

We were interested in studying the effects of MPs on sperm and oocyte function, as well as on oocyte proteomics. All of the functional data (i.e., sperm motility, sperm acrosomal integrity, sperm oxidative stress, sperm bead attachment, and oocyte maturation) consisted of percentages that ranged between 0 and 100. We therefore assessed the effects of MPs on these functional traits via generalised linear regression models with binomial error distributions. For the sperm oxidative stress, sperm bead attachment, and oocyte maturation, however, we used a quasibinomial error distribution to account for the fact that the data were under-dispersed. In addition, we also applied a hierarchical approach in which data from each bull and replicate were allowed to have randomly varying intercepts. The significance was checked using a Tukey HSD. Differences were considered significant when $p < 0.05$. All data analysis and visualization were carried out in R (ver. 4.2.1), and the scripts and packages used for carrying out our analyses are described in supplementary file S1 as well as on the GitHub repository https://github.com/NoonanM/MPs_and_Fertility.

bioRxiv preprint doi: https://doi.org/10.1101/2022.11.04.514813; this version posted November 4, 2022. The copyright holder for this preprint (which was not certified by peer review) is the author/funder, who has granted bioRxiv a license to display the preprint in perpetuity. It is made available under aCC-BY-ND 4.0 International license.

Statistical analysis of the proteomics data was done using R (4.2.1). Fold changes and p-value calculations were performed with the package MS-EmpiRe[70]. Proteins were considered significantly differentially abundant if adjusted p-value < 0.05. The differentially expressed proteins identified via these analyses are shown in Table 1. In addition, we used a random forest model to classify oocytes as belonging to either the control group, the 0.3 μm polystyrene bead treatment, or the 1.1 μm polystyrene bead treatment. The model was fit using the R package randomForest[73], using 20,000 trees, sampled with replacement, and five candidate genes were sampled at each split. We then evaluated the classification accuracy of the model and assessed the relative importance of the individual genes in overall model performance.

References

1. Cole, M., Lindeque, P., Halsband, C. & Galloway, T. S. Microplastics as contaminants in the marine environment: A review. *Mar. Pollut. Bull.* **62**, 2588–2597 (2011).
2. Rochman, C. M. & Hoellein, T. The global odyssey of plastic pollution. *Science* **368**, 1184–1185 (2020).
3. Free, C. M. *et al.* High-levels of microplastic pollution in a large, remote, mountain lake. *Mar. Pollut. Bull.* **85**, 156–163 (2014).
4. Lusher, A. L., Tirelli, V., O'Connor, I. & Officer, R. Microplastics in Arctic polar waters: The first reported values of particles in surface and sub-surface samples. *Sci. Rep.* **5**, 1–9 (2015).
5. Bergmann, M. *et al.* White and wonderful? Microplastics prevail in snow from the Alps to the Arctic. *Sci. Adv.* **5**, 1–11 (2019).
6. Osborne, M. In a First, Microplastics Are Found in Fresh Antarctic Snow. (2022). Available at: https://www.smithsonianmag.com/smart-news/in-a-first-microplastics-are-found-in-fresh-antarctic-snow-180980264/.
7. Carrington, D. Microplastics found in human blood for first time. (2022). Available at: https://www.theguardian.com/environment/2022/mar/24/microplastics-found-in-human-blood-for-first-time.
8. Parker, L. Microplastics are in our bodies. How much do they harm us? (2022). Available at: https://www.nationalgeographic.com/environment/article/microplastics-are-in-our-bodies-how-much-do-they-harm-us.
9. European Commission. *A European Strategy for Plastics in a Circular Economy. Communication from the Commission to the European Parliament, the Council, the European Economic and Social Committee and the Committee of the Regions*. (2018).
10. Rillig, M. C. & Lehmann, A. Microplastic in terrestrial ecosystems. *Science (80-.).* **368**, 1430–1431 (2020).
11. Grosberg, R. K., Vermeij, G. J. & Wainwright, P. C. Biodiversity in water and on land. *Curr. Biol.* **22**, R900–R903 (2012).
12. Hurley, R. R. & Nizzetto, L. Fate and occurrence of micro(nano)plastics in soils: Knowledge gaps and possible risks. *Curr. Opin. Environ. Sci. Heal.* **1**, 6–11 (2018).
13. de Souza Machado, A. A., Kloas, W., Zarfl, C., Hempel, S. & Rillig, M. C. Microplastics as an emerging threat to terrestrial ecosystems. *Glob. Chang. Biol.* **24**, 1405–1416 (2018).
14. Kaza, S., Yao, L. C., Bhada-Tata, P. & Van Woerden, F. *What a Waste 2.0: A Global Snapshot of Solid Waste Management to 2050*. **1999** □□□□ □□□□□ □□□□□□□□, (Washington, DC: World Bank, 2018).
15. Choi, B.-I., Harvey, A. J. & Green, M. P. Bisphenol A affects early bovine embryo development and metabolism that is negated by an oestrogen receptor inhibitor. *Sci. Rep.* **6**, 29318 (2016).

bioRxiv preprint doi: https://doi.org/10.1101/2022.11.04.514813; this version posted November 4, 2022. The copyright holder for this preprint (which was not certified by peer review) is the author/funder, who has granted bioRxiv a license to display the preprint in perpetuity. It is made available under aCC-BY-ND 4.0 International license.

16. Sone, K. *et al.* Effects of 17β-estradiol, nonylphenol, and bisphenol-A on developing Xenopus laevis embryos. *Gen. Comp. Endocrinol.* **138**, 228–236 (2004).
17. D'Angelo, S. & Meccariello, R. Microplastics: A Threat for Male Fertility. *Int. J. Environ. Res. Public Health* **18**, 2392 (2021).
18. Erdemir, F. *et al.* The effect of Sertraline, Paroxetine, Fluoxetine and Escitalopram on testicular tissue and oxidative stress parameters in rats. *Int. Braz J Urol* **40**, 100–108 (2014).
19. Stuppia, L., Franzago, M., Ballerini, P., Gatta, V. & Antonucci, I. Epigenetics and male reproduction: the consequences of paternal lifestyle on fertility, embryo development, and children lifetime health. *Clin. Epigenetics* **7**, 120 (2015).
20. Rattan, S. *et al.* Exposure to endocrine disruptors during adulthood: consequences for female fertility. *J. Endocrinol.* **233**, R109–R129 (2017).
21. Kumar, N., Sharan, S., Srivastava, S. & Roy, P. Assessment of estrogenic potential of diethyl phthalate in female reproductive system involving both genomic and non-genomic actions. *Reprod. Toxicol.* **49**, 12–26 (2014).
22. Du, Y.-Y. *et al.* Follicular fluid and urinary concentrations of phthalate metabolites among infertile women and associations with in vitro fertilization parameters. *Reprod. Toxicol.* **61**, 142–50 (2016).
23. Sussarellu, R. *et al.* Oyster reproduction is affected by exposure to polystyrene microplastics. *Proc. Natl. Acad. Sci.* **113**, 2430–2435 (2016).
24. Jin, H. *et al.* Polystyrene microplastics induced male reproductive toxicity in mice. *J. Hazard. Mater.* **401**, 123430 (2021).
25. Ijaz, M. U. *et al.* Dose-Dependent Effect of Polystyrene Microplastics on the Testicular Tissues of the Male Sprague Dawley Rats. *Dose-Response* **19**, 1–11 (2021).
26. Hou, B., Wang, F., Liu, T. & Wang, Z. Reproductive toxicity of polystyrene microplastics: In vivo experimental study on testicular toxicity in mice. *J. Hazard. Mater.* **405**, 124028 (2021).
27. Pimm, S. L. *et al.* The biodiversity of species and their rates of extinction, distribution, and protection. *Science (80-.).* **344**, (2014).
28. Ceballos, G. *et al.* Accelerated modern human-induced species losses: Entering the sixth mass extinction. *Sci. Adv.* **1**, 9–13 (2015).
29. Barnosky, A. D. *et al.* Has the Earth's sixth mass extinction already arrived? *Nature* **471**, 51–57 (2011).
30. Li, S. *et al.* Polystyrene microplastics induce blood–testis barrier disruption regulated by the MAPK-Nrf2 signaling pathway in rats. *Environ. Sci. Pollut. Res.* **28**, 47921–47931 (2021).
31. Deng, Y. *et al.* Enhanced reproductive toxicities induced by phthalates contaminated microplastics in male mice (Mus musculus). *J. Hazard. Mater.* **406**, 124644 (2021).
32. An, R. *et al.* Polystyrene microplastics cause granulosa cells apoptosis and fibrosis in ovary through oxidative stress in rats. *Toxicology* **449**, 152665 (2021).
33. Sussarellu, R. *et al.* Oyster reproduction is affected by exposure to polystyrene microplastics. *Proc. Natl. Acad. Sci.* **113**, 2430–2435 (2016).
34. Jaikumar, G., Brun, N. R., Vijver, M. G. & Bosker, T. Reproductive toxicity of primary and secondary microplastics to three cladocerans during chronic exposure. *Environ. Pollut.* **249**, 638–646 (2019).
35. Jeong, C.-B. *et al.* Microplastic Size-Dependent Toxicity, Oxidative Stress Induction, and p-JNK and p-p38 Activation in the Monogonont Rotifer (Brachionus koreanus). *Environ. Sci. Technol.* **50**, 8849–8857 (2016).
36. Au, S. Y., Bruce, T. F., Bridges, W. C. & Klaine, S. J. Responses of Hyalella azteca to acute and

bioRxiv preprint doi: https://doi.org/10.1101/2022.11.04.514813; this version posted November 4, 2022. The copyright holder for this preprint (which was not certified by peer review) is the author/funder, who has granted bioRxiv a license to display the preprint in perpetuity. It is made available under aCC-BY-ND 4.0 International license.

chronic microplastic exposures. *Environ. Toxicol. Chem.* **34**, 2564–2572 (2015).
37. Prata, J. C. *et al.* Preparation of biological samples for microplastic identification by Nile Red. *Sci. Total Environ.* **783**, 147065 (2021).
38. Collard, F., Gilbert, B., Eppe, G., Parmentier, E. & Das, K. Detection of Anthropogenic Particles in Fish Stomachs: An Isolation Method Adapted to Identification by Raman Spectroscopy. *Arch. Environ. Contam. Toxicol.* **69**, 331–339 (2015).
39. Braun, T. *et al.* Detection of microplastic in human placenta and meconium in a clinical setting. *Pharmaceutics* **13**, 1–12 (2021).
40. Pfohl, P. *et al.* Microplastic extraction protocols can impact the polymer structure. *Microplastics and Nanoplastics* **1**, 1–13 (2021).
41. Ibrahim, Y. S. *et al.* Detection of microplastics in human colectomy specimens. *JGH Open* **5**, 116–121 (2021).
42. Schwabl, P. *et al.* Detection of Various Microplastics in Human Stool. *Ann. Intern. Med.* **171**, 453 (2019).
43. Provencher, J. F. *et al.* Proceed with caution: The need to raise the publication bar for microplastics research. *Sci. Total Environ.* **748**, 141426 (2020).
44. Ivleva, N. P. Chemical Analysis of Microplastics and Nanoplastics: Challenges, Advanced Methods, and Perspectives. *Chem. Rev.* (2021). doi:10.1021/acs.chemrev.1c00178
45. Schymanski, D. *et al.* Analysis of microplastics in drinking water and other clean water samples with micro-Raman and micro-infrared spectroscopy: minimum requirements and best practice guidelines. *Anal. Bioanal. Chem.* **413**, 5969–5994 (2021).
46. Ragusa, A. *et al.* Plasticenta: First evidence of microplastics in human placenta. *Environ. Int.* **146**, 106274 (2021).
47. Jenner, L. C. *et al.* Detection of microplastics in human lung tissue using μFTIR spectroscopy. *Sci. Total Environ.* **831**, 154907 (2022).
48. Da Costa Filho, P. A. *et al.* Detection and characterization of small-sized microplastics (≥ 5 μm) in milk products. *Sci. Rep.* **11**, 1–13 (2021).
49. Leslie, H. A. *et al.* Discovery and quantification of plastic particle pollution in human blood. *Environ. Int.* **163**, 107199 (2022).
50. Veen, I. van der, Mourik, L. M. van, Velzen, M. J. M. van, Groenewoud, Q. R. & Leslie, H. A. *Plastic Particles in Livestock Feed , Milk , Meat and Blood*. (2022).
51. Liu, Z. *et al.* Polystyrene microplastics induced female reproductive toxicity in mice. *J. Hazard. Mater.* **424**, 127629 (2022).
52. Jiang, X. L. *et al.* Thioredoxin-interacting protein regulates glucose metabolism and improves the intracellular redox state in bovine oocytes during in vitro maturation. *Am. J. Physiol. - Endocrinol. Metab.* **318**, E405–E416 (2020).
53. Chu, Y. *et al.* Glutathione peroxidase-1 overexpression reduces oxidative stress, and improves pathology and proteome remodeling in the kidneys of old mice. *Aging Cell* **19**, 1–13 (2020).
54. García-Aguilar, A. & Cuezva, J. M. A Review of the Inhibition of the Mitochondrial ATP Synthase by IF1 in vivo: Reprogramming Energy Metabolism and Inducing Mitohormesis. *Front. Physiol.* **9**, (2018).
55. Kan, R. *et al.* Regulation of mouse oocyte microtubule and organelle dynamics by PADI6 and the cytoplasmic lattices. *Dev. Biol.* **350**, 311–322 (2011).
56. Yurttas, P. *et al.* Role for PADI6 and the cytoplasmic lattices in ribosomal storage in oocytes and translational control in the early mouse embryo. *Development* **135**, 2627–2636 (2008).
57. Wyatt, C. D. R. R. *et al.* A developmentally programmed splicing failure contributes to DNA

bioRxiv preprint doi: https://doi.org/10.1101/2022.11.04.514813; this version posted November 4, 2022. The copyright holder for this preprint (which was not certified by peer review) is the author/funder, who has granted bioRxiv a license to display the preprint in perpetuity. It is made available under aCC-BY-ND 4.0 International license.

damage response attenuation during mammalian zygotic genome activation. *Sci. Adv.* **8**, (2022).
58. Kasof, G. M., Goyal, L. & White, E. Btf, a Novel Death-Promoting Transcriptional Repressor That Interacts with Bcl-2-Related Proteins. *Mol. Cell. Biol.* **19**, 4390–4404 (1999).
59. Tang, C. *et al.* Tropomyosin-1 promotes cancer cell apoptosis via the p53-mediated mitochondrial pathway in renal cell carcinoma. *Oncol. Lett.* (2018). doi:10.3892/ol.2018.8204
60. Lee, H.-J. J. *et al.* AK2 activates a novel apoptotic pathway through formation of a complex with FADD and caspase-10. *Nat. Cell Biol.* **9**, 1303–1310 (2007).
61. Sutovsky, P. Proteomic analysis of mammalian gametes and sperm-oocyte interactions. *Soc. Reprod. Fertil. Suppl.* **66**, 103–16 (2009).
62. Lan, H., Lin, C. & Yuan, H. Knockdown of KRAB domain-associated protein 1 suppresses the proliferation, migration and invasion of thyroid cancer cells by regulating P68/DEAD box protein 5. *Bioengineered* **13**, 11945–11957 (2022).
63. Liu, Y.-H. H. *et al.* Heat shock protein 90α couples with the MAPK-signaling pathway to determine meiotic maturation of porcine oocytes1. *J. Anim. Sci.* **96**, 3358–3369 (2018).
64. Chen, W.-Y. *et al.* Heterogeneous nuclear ribonucleoprotein M associates with mTORC2 and regulates muscle differentiation. *Sci. Rep.* **7**, 41159 (2017).
65. Kogasaka, Y., Hoshino, Y., Hiradate, Y., Tanemura, K. & Sato, E. Distribution and association of mTOR with its cofactors, raptor and rictor, in cumulus cells and oocytes during meiotic maturation in mice. *Mol. Reprod. Dev.* **80**, 334–348 (2013).
66. Nolasco, S., Bellido, J., Gonçalves, J., Zabala, J. C. & Soares, H. Tubulin cofactor A gene silencing in mammalian cells induces changes in microtubule cytoskeleton, cell cycle arrest and cell death. *FEBS Lett.* **579**, 3515–3524 (2005).
67. Büks, F. & Kaupenjohann, M. Global concentrations of microplastics in soils – a review. *SOIL* **6**, 649–662 (2020).
68. Rillig, M. C. *et al.* About "Controls" in Pollution-Ecology Experiments in the Anthropocene. *Environ. Sci. Technol.* (2022). doi:10.1021/acs.est.2c05460
69. Tyanova, S., Temu, T. & Cox, J. The MaxQuant computational platform for mass spectrometry-based shotgun proteomics. *Nat. Protoc.* **11**, 2301–2319 (2016).
70. Ammar, C., Gruber, M., Csaba, G. & Zimmer, R. MS-EmpiRe Utilizes Peptide-level Noise Distributions for Ultra-sensitive Detection of Differentially Expressed Proteins. *Mol. Cell. Proteomics* **18**, 1880–1892 (2019).
71. de Castro, L. S. *et al.* Sperm Oxidative Stress Is Detrimental to Embryo Development: A Dose-Dependent Study Model and a New and More Sensitive Oxidative Status Evaluation. *Oxid. Med. Cell. Longev.* **2016**, 1–12 (2016).
72. Munnoł, K., Frond, H. De, O'Donnell, B. & Rochman, C. SLoPP and SLoPP-E Raman Spectral Libraries for Microplastics Research.
73. Liaw, A. & Wiener, M. Breiman and Cutler's Random Forests for Classification and Regression. *CRAN Repos.* (2018). doi:10.1023/A:1010933404324
74. Perez-Riverol, Y. *et al.* The PRIDE database resources in 2022: a hub for mass spectrometry-based proteomics evidences. *Nucleic Acids Res.* **50**, D543–D552 (2022).

bioRxiv preprint doi: https://doi.org/10.1101/2022.11.04.514813; this version posted November 4, 2022. The copyright holder for this preprint (which was not certified by peer review) is the author/funder, who has granted bioRxiv a license to display the preprint in perpetuity. It is made available under aCC-BY-ND 4.0 International license.

Acknowledgments

Funding: This research was supported by LMUexcellent, funded by the Federal Ministry of Education and Research (BMBF) and the Free State of Bavaria under the Excellence Strategy of the Federal Government and the Länder. MAMMF was also supported by the Alexander von Humboldt Foundation in the framework of the Sofja Kovalevskaja Award endowed by the German Federal Ministry of Education and Research. MJN was supported by NSERC Discovery Grant RGPIN-2021-02758. TT and SD were supported by Theramex Germany GmbH (SD).

Author contributions: Conceptualization: MAMMF; Methodology: MAMMF, NG, TF, JS, MJN and TT; Investigation: NG, RF, RR, JS; Supervision: MAMMF, MJN, TF, TT and SD; Writing—original draft: NG, MAMMF, MJN; Writing—review & editing: all authors.

Competing interests: Authors declare that they have no competing interests.

Data and materials availability: All data are available in the main text or the supplementary materials. The mass spectrometry proteomics data have been deposited to the ProteomeXchange Consortium via the PRIDE [74] partner repository with the dataset identifier PXD036415, accessible via: https://www.ebi.ac.uk/pride/ .

Supplementary Materials

Figure S1. Venn diagram for proteomics data of oocytes incubated with or without polystyrene microplastic beads for 24 h.
Data S1. All detected plastics with hit quality index (HQI) ≥ 75 for follicular fluid samples 1-3 and water controls 1 and 2.
Data S2. Differentially expressed proteins data for oocytes incubated with or without polystyrene microplastic beads for 24 h.
Data S3. List of all detected particles and their classification into non-plastic related particle (NP), plastic polymer (PP), pigment (PG), plasticizer (PZ), coating, solvent and fillers (CSF), or fiber (FB).
Table S1. Summary of Raman spectroscopy data for all samples.
Table S2. Density values of identified MPs for follicular fluid samples 1-3 and water controls 1 and 2.
File S1. R code used to generate the results and figures presented in the main text.